

[2,3]. For example, arcuate deltas are deposited by bed load or mixed load systems that bring large quantities of coarse material to the coastline as opposed to the elongate (birdfoot) deltas composed of large quantities of fine sediment deposited by a combination of suspended load and mixed load rivers. Methods initially developed for terrestrial systems will be used to gain information on the relationships between martian delta morphology, river regime, and coastal processes.

**References:** [1] Morgan J. P. (1970) *SEPM*, 15, 31-47. [2] Axelsson V. (1967) *Geogr. Ann.*, 49, 2-127. [3] Galloway W. E. (1975) *Houston Geol. Soc.*, 87-98.

**N94-33231**

*54-91 ABS ONLY*  
*3*  
*R*  
**CARBONATE FORMATION ON MARS: LATEST EXPERIMENTS.** S. K. Stephens<sup>1</sup>, D. J. Stevenson<sup>1</sup>, G. R. Rossman<sup>1</sup>, and L. F. Keyser<sup>2</sup>, <sup>1</sup>Division of Geological and Planetary Sciences, 170-25, California Institute of Technology, Pasadena CA 91125, USA, <sup>2</sup>Earth and Space Sciences Division, 183-901, Jet Propulsion Laboratory, California Institute of Technology, Pasadena CA 91109, USA.

**Introduction:** Laboratory simulations of martian CO<sub>2</sub> storage address a fundamental question about martian climate history: Could carbonate formation have reduced CO<sub>2</sub> pressure from a hypothetical >1 bar to the present 7 mbar in ≤3-4 b.y.? We address this problem with experiments and analysis [1,2] designed to verify and improve previous [3,4] kinetic measurements, reaction mechanisms, and product characterizations. Our theoretical modeling [5,6] has sought to improve existing models of martian CO<sub>2</sub> history [7-10], which generally assume an early CO<sub>2</sub> greenhouse atmosphere (questioned by Kasting [11]).

**Experimental Results:** A sensitive manometer monitored the pressure drop (PD) of CO<sub>2</sub> due to uptake by powdered silicate for periods of 3 to 100+ days. Initially we focused on monomineralic, crystalline samples, but more recently we ran basaltic glass (see Table 1). Grinding was done in a tungsten-carbide shatterbox. Di1 was not treated further, and all other monomineralic samples were

heated at 120°C for ~1 day after sitting in weak acetic acid for 1+ days. Bas was simply heated. Runs were performed at warm (25°C) and cold (-25°C) temperatures, about 1 bar CO<sub>2</sub> pressure, and specific surface areas of ~1 m<sup>2</sup>/g (~1 μm particles). Experiments included "vapor" (H<sub>2</sub>O premixed with CO<sub>2</sub>, for ~1-10 monolayer coverage), "damp" (H<sub>2</sub>O pipetted onto powder before soaking in), and "wet" (m<sub>H<sub>2</sub>O</sub> ~ m<sub>sample</sub>) runs.

BET specific surface areas were determined for Di1 and Bas, and quantitative results are given for experiments using these starting compositions (Table 2). Pressure drops (ΔP) for Di1 and Bas show rapid short-term (~1 day) CO<sub>2</sub> uptake and considerably slower long-term ΔP (Figs. 1 and 2). We know the changes are not due to H<sub>2</sub>O adsorption since there is always sufficient water to maintain a<sub>vap</sub>(H<sub>2</sub>O). However, we assume the short-term signal reflects CO<sub>2</sub> adsorption (consistent with previous measurements [7,12] and confirmed by desorption experiments). Curves for Di2, O11, and O12 are qualitatively similar to those for Di1, whereas Qtz and Plag show near-zero short-term ΔP and very slow long-term signal—indistinguishable from a leak (<10<sup>11</sup> mol/m<sup>2</sup>/s).

**Discussion:** Thermodynamic calculations [13] suggest that reactions should form carbonates from diopside and olivine, and possibly plagioclase, at martian P and T. PD results can be classified into three groups: diopsides and olivines, quartz and plagioclase, and basalt. Bas takes up more CO<sub>2</sub> than monomineralic, crystalline diopside, and olivine, despite the fact that it is probably >50% feldspar and quartz (i.e., relatively unreactive), suggesting a role for glass (vs. crystalline mineral).

No long-term ΔP was expected for Qtz (no cations), although adsorption was anticipated, while with Plag we expected a possible long-term signal, and again the absence of an adsorption effect was puzzling. One explanation involves the progressive polymerization of silicate tetrahedra: olivine (isolated tetrahedra) and pyroxene (chains) vs. feldspar and quartz (three-dimensional frameworks). The structure of olivine and diopside may make it easier for cations to physically adsorb (and/or chemically bond with) anions.

Also puzzling is the result of an X-ray photoelectron spectroscopy (XPS) analysis performed on Di2 exposed to similar P(CO<sub>2</sub>) and H<sub>2</sub>O vapor conditions as the PD experiment with Di1 (vapor)

TABLE 1. Minerals and rocks used for experimental samples.

| Sample                | Approximate Composition  | Sample Description  | Locale                 |
|-----------------------|--|---|------------------------|
| Diopside 1<br>[Di1]   | CaMgSi <sub>2</sub> O <sub>6</sub>   | Bulk, broken crystals,<br>~5% impurities  | Dog Lake, Quebec       |
| Diopside 2<br>[Di2]   | CaMgSi <sub>2</sub> O <sub>6</sub>   | Green, euhedral crystals,<br><2% impurities   | Rajasthan, India       |
| Olivine 1<br>[O11]    | Mg <sub>99</sub> Fe <sub>02</sub> SiO <sub>4</sub><br>[Forsterite 98%]   | Bulk, broken crystals,<br>~5% impurities  | Gabbs, Nevada          |
| Olivine 2<br>[O12]    | Mg <sub>88</sub> Fe <sub>12</sub> SiO <sub>4</sub>   | Translucent green pebbles (crystals),<br><2% impurities   | San Carlos, Arizona    |
| Quartz<br>[Qtz]       | SiO <sub>2</sub>   | Clear, euhedral crystal,<br><1% impurities  | Mt. Ida, Arkansas      |
| Plagioclase<br>[Plag] | Ab <sub>3</sub> An <sub>7</sub><br>[Ab = NaAlSi <sub>3</sub> O <sub>8</sub> ,<br>An = CaAl <sub>2</sub> Si <sub>2</sub> O <sub>8</sub> ] | Clear, euhedral crystal<br><1% impurities   | Ponderosa Mine, Oregon |
| Basalt<br>[Bas]       | Tholeiite<br>[50 wt% SiO <sub>2</sub> , 13% Al <sub>2</sub> O <sub>3</sub> ,<br>12% FeO, 9% MgO, 11% CaO]                                | ~98 wt% black glass, ~0.3 wt% dissolved H <sub>2</sub> O<br>~1 wt% crystals, 1991 lava flow,<br>quenched in air | Kilauea, Hawaii        |

TABLE 2. Conditions and results of PD experiments for Di1 and Bas.

| Experiment                 | A <sub>s</sub> <sup>*</sup><br>(m <sup>2</sup> /g) | P(CO <sub>2</sub> ) <sup>†</sup><br>(bars) | T<br>(°C) | H <sub>2</sub> O Content <sup>‡</sup><br>(Monolayers) | CO <sub>2</sub> Uptake<br>After 1 day <sup>§</sup><br>("Monolayers") | Rate of CO <sub>2</sub> Uptake <sup>¶</sup>             |       |          |
|----------------------------|--|--|-----------|---|--|---|-------|----------|
|                            |  |  |           |   |  | Day 3<br>(10 <sup>11</sup> Molecules/m <sup>2</sup> /s) | Day 7 | >20 Days |
| Di1 (crystalline)          |  |  |           |   |  |   |       |          |
| Cold <sup>**</sup> , vapor | 3  | 0.96                                       | -25       | 1   | 0.2  | 20  | 15    | <3       |
| Warm, damp                 | 3  | 0.96                                       | 25        | 200   | 1.7  | 50  | 25    | <6       |
| Warm, wet                  | 3  | 0.96                                       | 25        | 1000  | 3.6  | 60  | —     | —        |
| Bas (glass)                |  |  |           |   |  |   |       |          |
| Warm, vapor <sup>**</sup>  | 0.6  | 0.96                                       | 25        | 20  | 1.5  | 50  | 20    | —        |
| Warm, ~damp                | 0.6  | 0.96                                       | 25        | 300   | 3.0  | 70  | —     | —        |
| Warm, damp                 | 0.6  | 0.96                                       | 25        | 1000  | 5.5  | 120   | —     | —        |

\* BET specific surface area, measured using Ar and Kr adsorption.

† CO<sub>2</sub> pressure at start of run, not corrected for pressure drop over a period of days.

‡ Surface depth of water film for given A<sub>s</sub> and ~10 Å<sup>2</sup> per H<sub>2</sub>O molecule, in equivalent monolayers.

§ Surface depth of gas, assuming ~20 Å<sup>2</sup> per CO<sub>2</sub> molecule, all deposited on sample.

¶ Equivalent to rates of inferred carbonate formation.

\*\* Data shown for cold (-25°C) portions of run only; warm (25°C) intervals were also monitored.

\*\* H<sub>2</sub>O content may be up to twice the number shown due to ~0.3 wt% dissolved H<sub>2</sub>O in basalt glass.

shown in Table 2. Although conducted at +25°C, the XPS experiment yielded no added carbonate on a freshly cleaved crystal surface, implying no significant bound reaction product. This might be due to a different surface texture or degree of fracturing compared to a powder.

From the dependence of CO<sub>2</sub> uptake on temperature and water content (Table 2, Figs. 1 and 2), we verified that "warm and wet" PD conditions store considerably more CO<sub>2</sub> than "cold and dry." For scenarios involving liquid water, CO<sub>2</sub> uptake is consistent with the formation of a monolayer of carbonate in ~10–100 days. The asymptotic decrease in the rate of uptake could represent the continuation of chemistry beyond the surface reaction that takes place as a monolayer of carbonate is formed [6], although it is interesting that initial CO<sub>2</sub> uptake is always of the order of 1 monolayer. Long-term

uptake rates are comparable to those obtained by Booth [4], 10<sup>11</sup>–10<sup>12</sup> mol/m<sup>2</sup>/s. However, Booth inferred carbonate formation by evolving CO<sub>2</sub> at the end of runs, assumed no limitation due to diffusion through a product layer (indeed, «1 monolayer was inferred to have formed), and concluded that reactions depended on ionic reactions in a thin, approximately monolayer H<sub>2</sub>O film at the high-T end of a cycle in temperature. Our results then are not directly comparable: we have considerably more water, higher temperatures, and no cycling, and we infer (from monitored PD experiments) nonreversible formation of about 1 monolayer of carbonate.

An extrapolation from long-term CO<sub>2</sub> uptake rates (Table 2) shows that an upper limit of 1–5 mbar/yr (at least for experimental P, T, and H<sub>2</sub>O content, and for timescales on the order of months) can be taken up by a Bas regolith 100 m in thickness and covering

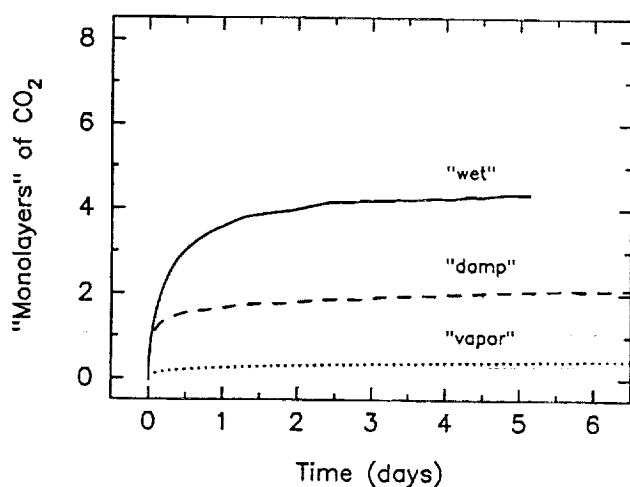


Fig. 1. PD results for Di1 (crystalline). A<sub>s</sub> = 3 m<sup>2</sup>/g (see Table 2). Minor fluctuations in PD are due to small T changes.

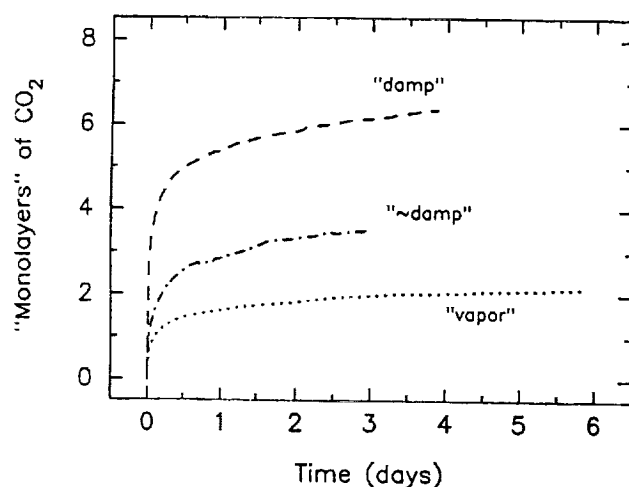


Fig. 2. PD results for Bas (glass). A<sub>s</sub> = 0.6 m<sup>2</sup>/g (see Table 2).

the surface of Mars. Modeling of nonaqueous, diffusion-limited growth of carbonate rinds [6] has established that, if long-term kinetics are anywhere near the laboratory rates implied by Booth and now by us, then the growth rate will decrease rapidly after a few 100 m.y. and we may require times approaching 3–4 b.y. to store 1 bar of CO<sub>2</sub> on Mars.

**References:** [1] Stephens S. K. et al. (1992) *LPI Tech. Rpt. 92-04*, 34–36. [2] Stephens S. K. et al. (1992) *Bull. A.A.S.*, 24, 980. [3] Booth M. C. and Kieffer H. H. (1978) *JGR*, 83, 1809–1815. [4] Booth M. C. (1980) Ph.D. thesis, UCLA. [5] Stephens S. K. and Stevenson D. J. (1990) *LPS XXI*, 1198–1199. [6] Stephens S. K. and Stevenson D. J. (1992) *LPI Tech. Rpt. 92-02*, 136–137. [7] Fanale F. P. et al. (1982) *Icarus*, 50, 381–407. [8] Kahn R. (1985) *Icarus*, 62, 175–190. [9] Pollack J. B. et al. (1987) *Icarus*, 71, 203–224. [10] Haberle R. M. et al. (1993) *LPI Tech. Rpt. 93-03*, 13–14. [11] Kasting J. F. (1991) *Icarus*, 94, 1–13. [12] Zent A. P. et al. (1987) *Icarus*, 71, 241–249. [13] Gooding J. L. (1978) *Icarus*, 33, 483–513.

## N94-33232

542-91 ABS. ONLY  
8-2  
**GEOLOGIC CONTROLS OF EROSION AND SEDIMENTATION ON MARS.** K. L. Tanaka<sup>1</sup>, J. M. Dohm<sup>1</sup>, and M. H. Carr<sup>2</sup>, <sup>1</sup>U.S. Geological Survey, Flagstaff AZ 86001, USA, <sup>2</sup>U.S. Geological Survey, Menlo Park CA 94305, USA.

Because Mars has had a history of diverse erosional and depositional styles, an array of erosional landforms and sedimentary deposits can be seen on Viking orbiter images. Here we review how geologic processes involving rock, water, and structure have controlled erosion and sedimentation on Mars, and how further studies will help refine our understanding of these processes.

**Impacts:** The early geologic record is dominated by large impacts, including dozens of circular basins that exceed 200 km in diameter [1,2]. Large impact events have strongly influenced erosional and sedimentary processes throughout Mars' geologic history by (1) comminuting crustal rocks into very poorly sorted debris [3]; (2) forming large topographic basins whose rims have been eroded and whose interiors have accumulated sediment (and, in some cases, temporary lakes) [4,5]; and (3) seismically disrupting [6] and driving hydrothermal circulation [7] in aquifers. Large volumes of sediment are contained in Argyre and Hellas Basins and the northern plains, which include several large impact basins and one proposed mega-impact, the 7700-km-diameter Borealis Basin [1,8].

**Tectonism:** For Earth, sedimentologists have said that "the major control of all sedimentation is tectonics" [9]. For Mars, tectonism has also been a major sedimentological control in that it has (1) produced topographic relief, (2) provided fractures that have served as zones of enhanced surface erosion, as well as subsurface conduits for the flow of water, and (3) produced seismicity. Possible tectonic lowering of the northern lowlands at the end of the Noachian Period may have caused the extensive erosion observed there and along the highland/lowland boundary [10,11]. This erosion formed vast areas of knobby terrain in the lowlands and fretted terrain and channels along the lowland boundary. In addition, the increased surficial activity appears to have been associated with a climate change that resulted in waning highland erosion [11,12]. Also, contemporaneous deformation of the Thaumasia highlands by folding and faulting led to local channel formation [e.g., 13].

The growth of Tharsis and Valles Marineris, which may have peaked in Late Hesperian time, resulted in high local to regional relief, as well as possible changes in axial orientation of the planet [14] and high obliquities [15]. In addition, this tectonism led to catastrophic flooding of the Chryse region [16] and of Mangala Valles [17] and possibly to the formation of small channels along the edge of the Thaumasia plateau [18]. This flooding also may have led to temporary climate change [19] that caused glaciation in the southern high latitudes [20].

**Volcanism:** Mars is renowned for its huge volcanic shields and extensive lava fields. Volcanism (and intrusion) apparently occurred throughout geologic time [21,22]. Their influences on erosion include (1) formation of topographic highs, (2) local production of easily erodible pyroclastic material [23], (3) local rises in crustal temperature, leading to increased hydrothermal circulation, and (4) local disruption of near-surface rocks. In the Tharsis region, many of these effects were associated with tectonism.

**Crustal Ground Water and Ground Ice:** The presence of large volumes of water and ice in the martian crust has been the major factor in producing the large-scale erosion evidenced by various landforms. At present, interstitial or massive ice may be common in the upper kilometer or so of the crust where freezing temperatures exist, particularly at high latitudes [24]. Steep slopes in ice-rich material may lead to the formation of debris aprons and rock glaciers. Perched subpermafrost aquifers (that may have provided pore water for sapping and catastrophic discharges) and ice-laden permafrost zones could have been charged from the water table by thermal liquid or vapor transport and by seismic pumping [25].

**Eolian Activity:** The transport by wind of dust and sand-sized particles on the martian surface is shown by extensive dune fields in the the north polar region and within local topographic traps [26] and by polar layered deposits and mantle material [27]. Moreover, winds can erode friable materials, producing the yardangs and deflation pits that are common in extensive equatorial deposits in the Medusae Fossae region. Ephemeral wind streaks all over Mars attest to the ongoing eolian transport of fine particles.

**Future Work:** Through geologic mapping of Mars at local (1:500,000) and regional (1:2,000,000 and 1:5,000,000) scales and by topical studies, workers have continued to assess the geologic settings and processes that have caused erosion and sedimentation on Mars. Detailed maps have been made of the Tharsis volcano-tectonic region, the Elysium volcanics and channels, the Chryse channels and basin, the Hellas and Argyre basins, the Valles Marineris, Lunae Planum, Mangala Valles, and other regions. These maps provide the basis for more rigorous semiquantitative analyses of Mars' sedimentological history. To achieve this, we plan to augment the mapping studies with further research and compilation. Our objectives include (1) statistical studies of martian channels, including their morphology (lengths, type, drainage pattern, junction angles, etc.) and their distribution by age, elevation, slope, and geologic setting, and (2) determination of the intensities of erosional events along the highland/lowland boundary and their relation to infilling of the northern plains.

We have recently completed a digitized, vector-format, graphical database of channels on Mars as observed on the 1:2,000,000-scale photomosaic series. We plan to implement GIS software and merge other Mars databases (e.g., geology and topography) to accomplish our objectives. This approach will permit evaluation of